NISTIR 7814

Report on VAMAS Round Robin of ISO 13067: Microbeam analysis – Electron backscatter diffraction – Measurement of average grain size

Adam Creuziger
Mark Vaudin

National Institute of Standards and Technology
U.S. Department of Commerce

NISTIR 7814

Report on VAMAS Round Robin of ISO 13067: Microbeam analysis – Electron backscatter diffraction – Measurement of average grain size

Adam Creuziger
Guest Researcher
Metallurgy Division
Material Measurement Lab
Kent State University

Mark Vaudin
Ceramics Division
Material Measurement Lab

September 2011

U.S. Department of Commerce
Rebecca M. Blank, Acting Secretary

National Institute of Standards and Technology
Patrick D. Gallagher, Under Secretary for Standards and Technology and Director

Abstract

NIST recently participated in a Versailles Project on Advanced Materials and Standards (VAMAS) sponsored round robin evaluation of a new ISO document draft, ISO 13067: Microbeam analysis – Electron backscatter diffraction – Measurement of average grain size. This report details the results of the study, some of the difficulties encountered and suggestions to improve the ISO document. The average grain size measured using this technique was internally consistent within NIST and compared well to the preliminary aggregate round robin data revealed to the authors. The methods described in ISO 13067 to modify or 'clean up' the raw data were found to significantly affect the average grain size value.

Background

In April of 2010, the authors were approached about participating in a round robin evaluation of a draft International Organization for Standardization (ISO) document created by ISO technical committee (TC) 202. This document is ISO 13067: Microbeam analysis – Electron backscatter diffraction – Measurement of average grain size [1]. The Versailles Project on Advanced Materials and Standards (VAMAS) would coordinate the round robin under Technical Working Area (TWA) 37, Quantitative Microstructural Analysis. An alternate standard for grain size measurement using electron backscatter diffraction (EBSD) is also available as ASTM E2627: Standard Practice for Determining Average Grain Size Using Electron Backscatter Diffraction (EBSD) in Fully Recrystallized Polycrystalline Materials [2].

Prior standard methods for average grain size measurement using light microscopy are available. Standards such as ASTM E112: Standard Test Methods for Determining Average Grain Size [3] have been published since the 1950's and are frequently used for grain size analysis. However, there are difficulties with this and similar techniques.

Conventional grain size analysis requires etching of a polished sample to reveal the grain structure. Finding a suitable etchant can be a non-trivial task. The ideal etchant would evenly etch all grain boundaries and be safe for the user. Real etchant solutions typically only attack certain types of grain boundaries or are otherwise dangerous to use. There is also the difficulty in determining the type of grain boundary. There are many different types of grain boundaries that can have particular properties: high angle, low angle, twin, coincident site lattices (CSL). Usually these structures cannot be distinguished by etching alone and may be types of grain boundaries to disregard in an average grain size measurement.

Grain size analysis methods based upon electron backscatter diffraction (EBSD) can be used to overcome some of these difficulties. One of the most significant is that the sample does not need to be etched. The EBSD method provides crystallographic orientation data at a series of points. The orientation difference between adjacent points can be used to define a grain boundary. In this way the definition of a grain boundary is applied uniformly throughout the sample. Crystallographic and sample boundary relations can be used to determine other grain boundary types. The crystallography information can also be used as phase discrimination as well. There are some disadvantages of EBSD, namely the

requirement of a scanning electron microscope (SEM) with EBSD equipment for automated indexing. The surface preparation is also more stringent, as the EBSD technique requires the surface 50 nm to 100 nm to have diffracting lattice planes. This often requires chemo-mechanical polishing or electrolytic polishing to remove any deformation caused by mechanical polishing on the surface.

Methods

Samples

Dr. Kenneth Mingard at the National Physical Laboratory (NPL) in the United Kingdom provided two 13 mm diameter commercial purity α-phase (hexagonal) Ti samples for our investigations. The samples were labeled, sectioned, polished and electropolished prior to arrival. Two microindents were made in the surface of the sample, one on the edge for orientation and one in the center. The round robin requested that the authors analyze regions within 5 mm of the center indent, and that five test regions should be scanned on each sample.

Data Acquisition

Two different scanning electron microscopes (SEMs) were used in this study: a Hitachi S-4700[1] and a JEOL 6400. The Hitachi S-4700 is a cold tip field-emission gun SEM (FEG-SEM) while the JEOL 6400 is a thermionic emission SEM with a LaB_6 cathode. Both SEMs are equipped with an Oxford Instruments Nordlys II detector and an HKL Channel 5 software package for EBSD analysis (version 5.0.9.0).

As per ISO 13067, the SEM magnification was calibrated at various times during the study according to ISO 16700: Microbeam analysis – Scanning electron microscopy – Guidelines for calibrating image magnification [3], using National Institute of Standards and Technology (NIST) Reference Material (RM) 8820 [4]. The final calibrations for each instrument are recorded in Table 1. In working with the manufacturer, the authors determined that significant scan instabilities could result unless the Hitachi SEM was set to a 'slow scan' mode during the EBSD data collection process. These results have underscored the need to check the magnification calibration and scan generation of the SEMs before collecting data.

The scan employed by the authors was 400 pixels x 400 pixels with a step size of 2.5 μm. At each point in a scan, the software automatically obtained an electron backscatter diffraction pattern (EBSP) and determined the position of diffraction bands. From the band location pattern the orientation of the diffracting planes at the analysis point and the angles between the diffracting planes were determined. From the interplanar angles, the crystallographic orientation at the analysis point was determined. More information on the EBSD technique can be found in [5].

---

[1] "Certain commercial equipment, instruments, or materials are identified in this paper in order to specify the experimental procedure adequately. Such identification is not intended to imply recommendation or endorsement by the National Institute of Standards and Technology, nor is it intended to imply that the materials or equipment identified are necessarily the best available for the purpose."

The Hitachi software had access to the PDF2 database [6] and the NIST Structural Database [7], which contained a variety of different α-phase Ti lattice parameters. After comparing the pattern fits, the Ti-JOMTAA [8] parameters or Ti-PPSOAU [9] parameters were found to improve the hit rate (ratio of successfully indexed pixels to total pixels investigated) by approximately 5% over the parameters in the HKL database. The unit cells from each of these files are given in Table 2. The JEOL system did not have access to the PDF2 database, so a database entry was generated using the HKL software program Twist with Wyckoff positions of (1/3, 2/3, 1/4) and space group 194.

Before each scan, it was necessary to adjust the EBSD calibration parameters in the HKL EBSD capture software (Flamenco) to obtain the high hit rate (>90%) required by ISO 13067. If the steps described below were not carried out between data scans or if the stage were moved to a different location on the sample, the hit rate would decrease by 10% to 30%. The sample working distance was adjusted such that the highest intensity spot was in the center of the phosphor screen. A new background was collected, and the EBSD geometry was adjusted so the region of interest (ROI) circle captured the well-defined portion of the Kikuchi pattern. Then the EBSD calibration was refined to set the detector geometry in Flamenco.

After calibrating the EBSD system, the scan parameters were varied to determine optimal settings for both microscopes. The scan parameters used for our analysis are listed in Appendix A. Most of these parameters were determined iteratively or with assistance from the manufacturer. Increasing the maximum number of bands from 5 to 6 lead to a decrease in hit rate, as did low or normal divergence. The authors also wanted to minimize the time it took to acquire the data sets, which lead to our choices for acquisition time, pattern binning, number of frames to average, Hough resolution, and number of reflectors. Using a single frame was too noisy for reliable indexing, but averaging more than two frames did not further improve indexing. The data collection scan was 160 000 pixels; the average duration for the JEOL SEM was 3 h 22 min and for the Hitachi it was 1 h 40min.

Data Analysis

Figure 1 shows the raw data from a typical scan, with coloration corresponding to the Euler angles of each pixel. After acquisition of the data, data cleaning operations were conducted prior to determination the grain size. To summarize ISO 13067, there are three parts to the data cleaning operation: removal of small grains; filling in unindexed pixels; and setting a minimum grain size for grain size analysis. The complete procedure the authors used for data cleaning is listed in Appendix B and includes information about the images recorded for the VAMAS report sheets. The median recommended value from ISO 13067 for smallest grains (4) was used, so all grains less than four pixels were nullified and set to zero solution. After this, a threshold of 5 nearest neighbors or more was used for cleanup of the dataset, so that all zero solution data points with five nearest neighbors or more of a common orientation were filled in with the average orientation. This value for nearest neighbors was chosen from the constraints in the ISO document: that the number of pixels modified should not exceed 5% of the data set; the fill

should not be done iteratively; and the grains should not have obvious holes in them. After this, grains smaller than ten pixels were removed from the grain size analysis.

A consideration in determining the grain size in these samples was pseudosymmetry, defined in ISO 13067 as the potential for an EBSD pattern to be indexed in several different ways due to internal similarities within the EBSD pattern that are not caused by crystal symmetry. The authors noted that in the Euler angle maps some regions that appeared to be a single grain would have a number of points of a different orientation within the apparent single grain. The authors determined that the only difference in orientation between these pixels was that the c and a axes were interchanged. These pseudosymmetries were best categorized by analyzing the misorientations between adjacent pixels. Figure 2 is an example of a misorientation angle density plot. Each spike in this plot is an over-representation of a specific misorientation angle. Misorientation axes corresponding to these misorientation angles were analyzed by plotting in an inverse pole figure the misorientations axes for a small range of angles around the spike in misorientation angle density, as shown in Figure 3. From these plots and detailed examination of our data sets, ten pseudosymmetry operators were found, as listed in Table 3. Only four pseudosymmetry operators were found to affect the grain size measurements; the other pseudosymmetry operators did not occur in large enough groups to remain after data cleaning operations.

Equivalent circle diameter and grain area were directly calculated in Tango (the HKL EBSD map plotting software). The linear intercept values requested in the VAMAS report were not calclated by Tango. A script in the statistical computing software, R, was written to calculate linear intercept values and relevant statistics. The equation to calculate the linear intercept (LI) value is given in ISO 13067 [1]. This script also checked the average values for equivalent circle diameter and grain area from Tango against those calculated in R, and they were found to be in agreement.

Results

Average Grain Size

Data were collected from five areas on both of the Ti samples, all within 5 mm from the central indent. The results reported to the VAMAS round robin are summarized in Table 4 to Table 7. Table 4 lists the mean circle equivalent grain size for sample 23. Table 5 lists the mean linear intercept values for sample 23. Table 6 and Table 7 respectively describe the mean circle equivalent grain size and mean linear intercept values for sample 24. The unweighted average and standard deviation are the simple averages of the mean grain size and standard deviation of the average grain size for the five data sets recorded. The final column is the mean of the full data set, which creates a larger set from each of the five individual grain size measurements, and the mean value is computed from the large dataset. There is a discrepancy between the mean of the full data set and the unweighted average, due

to the different number of grains in each data set. However, an average weighted by the number of grains matches the mean of the full data set.

A variety of different data cleaning methods was investigated before choosing the parameters discussed in the data analysis section. Figure 4 and Figure 5 show some of these data cleaning methods and the effect they had on the grain size statistics. These figures will be discussed in more detail below.

Uncertainty

As currently written, ISO 13067 gives very little guidance as to uncertainty analysis. ISO 13067 states, "The uncertainty shall be determined with reference to the Guide to the Expression of Uncertainty in Measurement. ISO/TS 21748:2008." A few factors to consider follow in the text of the standard (linear calibration, resolution, step size, post-acquisition treatment of raw data, tilt, specimen drift), but no references or guides are given as to how to properly account for them for EBSD methods or integrate them into an aggregate uncertainty metric. At this time, the authors have only attempted to assess the uncertainty in specimen drift, tilt error and linear calibration.

The linear calibration errors are shown in Table 1. As shown, the Hitachi may overestimate the grain size area by 2.1%, while the JEOL may underestimate the area by 4.1%. The tilt was assessed by measuring RM8820 at the nominal 70° tilt used for EBSD. For both the Hitachi and JEOL, the measured value was 69.8°. This 0.2° deviation results in a shortening perpendicular to the tilt axis of 1%. To assess the specimen drift, images were automatically recorded before and after acquisition. Image subtraction of these images did not show any systematic shifting of the image within the resolution of the SEM image, which was 1.76 μm per pixel.

Noise Reduction Methods

Figure 4 shows some of the effects of noise reduction methods and the initial minimum grain size (section 6.3.1 in ISO 13067). The majority of grains in the raw data set are individual pixels (5191 grains of the 6479 grains detected in the raw data were 1 pixel in area). Removing (removed pixels are set to zero solution) single pixels from the average grain size calculation increases the circle equivalent diameter from 6.64 μm to 23.4 μm. Increasing the initial minimum grain size up to ≤4 pixels produces more modest increases, up to 31.1 μm for ≤4 pixels. At this point, how to translate the choice of initial minimum grain size into a reasonable metric for uncertainty is not clear, but the effect would be a bias error.

After the initial minimum grains are removed, zero solution points are filled in with orientations adjacent to the point, referred to as noise reduction. ISO 13067 recommends avoiding iterative noise reduction methods. For the noise reduction methods used here, points that have no solution are evaluated to determine the number of nearest neighbors (NN). This value can range between 1 and 8, since the data are recorded in a rectilinear grid. For non-iterative noise reduction, one value along this range of nearest neighbors is chosen, and any points that have no solution are filled if they have that value of nearest neighbors or more. Three different NN

values were investigated: 1, 5, and 7. For example, in the NN=7 case, only zero solution points that had 7 indexed points surrounding the zero solution point are filled in with the average orientation of those 7 points. The grain size increased as the number of nearest neighbors decreased. In addition, a sequential iterative method was also performed, sequentially decreasing the NN value from 8 to 4 while iterating each noise reduction step until there were no more points with that number of nearest neighbors. The grain size calculated from the iterative sequential method is between the grain sizes calculated from the 5 and 1 nearest neighbor methods. Similar to the effect of minimum initial grain size, the authors are not sure how to translate these data into a reasonable metric for uncertainty. The effects of resolution and step size on the uncertainty were not addressed.

After the initial minimum grain size and the noise reduction using nearest neighbors, an additional minimum grain size of 10 pixels is applied (ISO 13067 section 6.3.4). All grains 10 pixels or less are removed from the average grain size measurement. While this step may seem redundant to the initial minimum grain size grain size, the authors have noted that after noise reduction, grains less than 4 pixels are created. The 10 pixels cut off was recommended in ISO 13067 due to pixelation errors. However, as Figure 5 shows, the average grain size increases nearly linearly for each pixel in the final minimum grain cutoff, introducing the possibility of another bias error.

Discussion

The results of our analysis were self-consistent, with a grain size average of about 33 μm. An average grain contains approximately 130 pixels, calculated from the average grain size and step size. Only one analysis might be considered an outlier (sample 24, JEOL area 1) leading to a larger standard deviation for that series than the other three. The other three data sets had standard deviations of about 1 μm to 2 μm. There was consistency both between the samples and between the equipment used. From the preliminary aggregate round robin data revealed to us, our values also compare well with the mean values of the round robin.

However, it is the opinion of the authors that the uncertainty analysis for the ISO needs improvement. As mentioned in the results, several contributions to the uncertainty have not been assessed, and how to assess them is not clear. The choices for minimum grain size cutoff and noise reduction methods leave the final numbers for average grain size dependent on these choices and may create bias errors.

Related to the uncertainty analysis, different noise reduction methods can lead to different values for the average grain size. For the noise reduction methods investigated, different numbers of nearest neighbors create average grain sizes that differ by 3 μm. In addition, with a non iterative method, some grains in the sample have regions of zero solutions interior to the grain boundary, even after noise reduction. The authors have also noted that the noise reduction method can create grains smaller than the initial minimum grain size. For example, often 1 pixel square grains are created after noise reduction. It is not clear why this occurs.

Neither ISO 13067 nor ASTM E2627 explicitly requires repeated measurements such as those performed as part of the round robin. Without repeated measurements, the uncertainty can only be determined by an analysis of the scatter in the data. A typical distribution of the grain size is shown in Figure 6, with a mean and standard deviation of 34.53 μm ± 15.83 μm. As written, both ISO 13067 and ASTM E2627 base the uncertainty on the dispersion of the grain size in a single sample, not the uncertainty in repeated average measurements. Using this definition, the uncertainty for a sample from this data set would be on the order of 15 μm, which does not seem to be the goal of either standard.

In contrast, the method in ASTM E112: Standard Test Measurements for Determining Average Grain Size provides an average value on a line or circle. These averages are then used to calculate the uncertainty on the average value, but only the average value, not any metrics on the distribution of grain sizes. A similar metric for Gaussian distributions is the standard deviation of the mean, which is the standard deviation divided by the square root of the number of samples [10]. For the distribution shown in Figure 6 the standard deviation of the mean is ±0.51 μm. This value is closer in magnitude to the uncertainty from repeated measurements and may be the metric intended. A further question is the applicability of a mean, standard deviation and standard deviation of the mean values on a distribution that does not follow a Gaussian distribution. Viewing the histogram in Figure 6, it is clear that this is not a normal distribution, but possibly closer to a log-normal or Weibull distribution. Perhaps metrics that describe the functional form of the distribution would be more useful in predicting material properties than a mean grain size.

There are other opportunities for the EBSD technique that are not currently utilized in ISO 13067. By measuring the distribution of grain sizes in the test area, not just a simple average value, there is more information in the data set than an average value. Often the largest or smallest grains dominate some material properties, and measurements of the distribution can provide information about these grain sizes. The authors recommend that any subsequent revisions of ISO 13067 consider reporting the distribution in grain size instead of focusing on an average value. These and other comments to improve ISO 13067 will be provided to the ISO TC and are listed in Appendix C.

Conclusions

ISO 13067: 'Microbeam analysis – Electron backscatter diffraction – Measurement of average grain size' advances measurements of grain size to allow for a less ambiguous definition of a grain. Obtaining EBSD maps of high enough quality to meet this standard is a challenge, and may be very difficult for novice users. A revision of this standard or a new standard that focuses on the distribution of the grain sizes should be considered to utilize the discrete grain size data currently recorded by the EBSD maps, but only used in ISO 13067 to calculate a mean value. The uncertainty analysis section of ISO 13067 should be improved. As written, it is unclear if the uncertainty is to be estimated by repeated measurements

or a single measurement. More details on how to integrate data cleaning operations into the uncertainty are also needed.

Acknowledgements

The authors would like to thank Dr. Kenneth Mingard and Dr. Peter Quested of the National Physical Laboratory (NPL) in the UK for inviting us to participate in the round robin and for providing the Ti samples; Dr. John Bonevich, Director of the Metallurgy/Ceramics Microscopy Lab for advice and assistance with the microscopes; Scott Sitzman of Oxford Instruments for advice and assistance with the HKL software package; and William Luecke for many useful discussions.

References

[1] ISO FDIS 13067: Microbeam Analysis – Electron Backscatter Diffraction – Measurement of average grain size. 2011. International Organization for Standardization.

[2] ASTM E2627: Standard Practice for Determining Average Grain Size Using Electron Backscatter Diffraction (EBSD) in Fully Recrystallized Polycrystalline Materials. 2010. ASTM International.

[3] ASTM E112: Standard Test Methods for Determining Average Grain Size. 2004. ASTM InternationalISO 16700: Microbeam analysis – Scanning electron microscopy – Guidelines for calibrating image magnification. 2004. International Organization for Standardization.

[4] National Institute of Standards and Technology Report of Investigation Reference Materials 8820: Scanning Electron Microscope Scale Calibration Artifact. 2009. URL: http://www.nist.gov/srm/index.cfm

[5] Introduction to Texture Analysis 2nd Ed. O. Engler and V. Randle CRC Press 2010

[6] Powder Diffraction File. PDF2_2002 database. International Centre for Diffraction Data http://www.icdd.com/products/pdf2.htm

[7] NIST Structural Database. National Insitute of Standards and Technology http://www.nist.gov/srd/nist83.cfm

[8] H. T. Clark, Jr. "The lattice Parameters of High Purity Alpha Titanium; and the Effects of Oxygen and Nitrogen on Them" Journal of Metals (1949), vol 1, p588

[9] R. M. Wood. "The Lattice Constants of High Purity Alpha Titanium" Proceedings of the Physical Society, London, (1962), vol. 80, page 783

[10] Joint Committee for Guides in Metrology. "Evaluation of measurement data – Guide to the expression of uncertainty in measurement." URL: http://www.bipm.org/en/publications/guides/gum.html

Figures

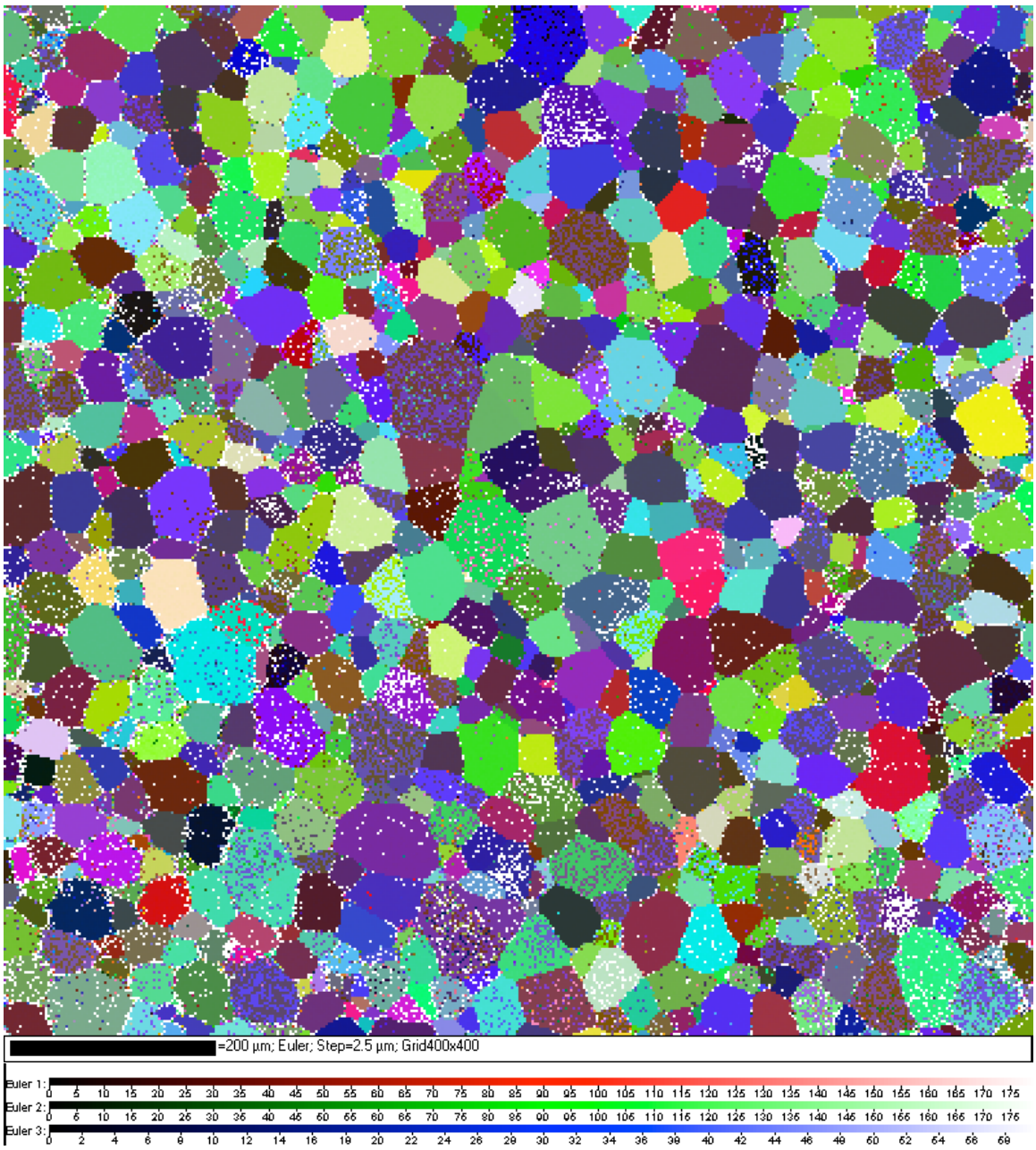

Figure 1: Raw Data from EBSD map. The colors correspond to the Euler angles listed in the key above. Data is from JEOL data set, sample 24, scan 1.

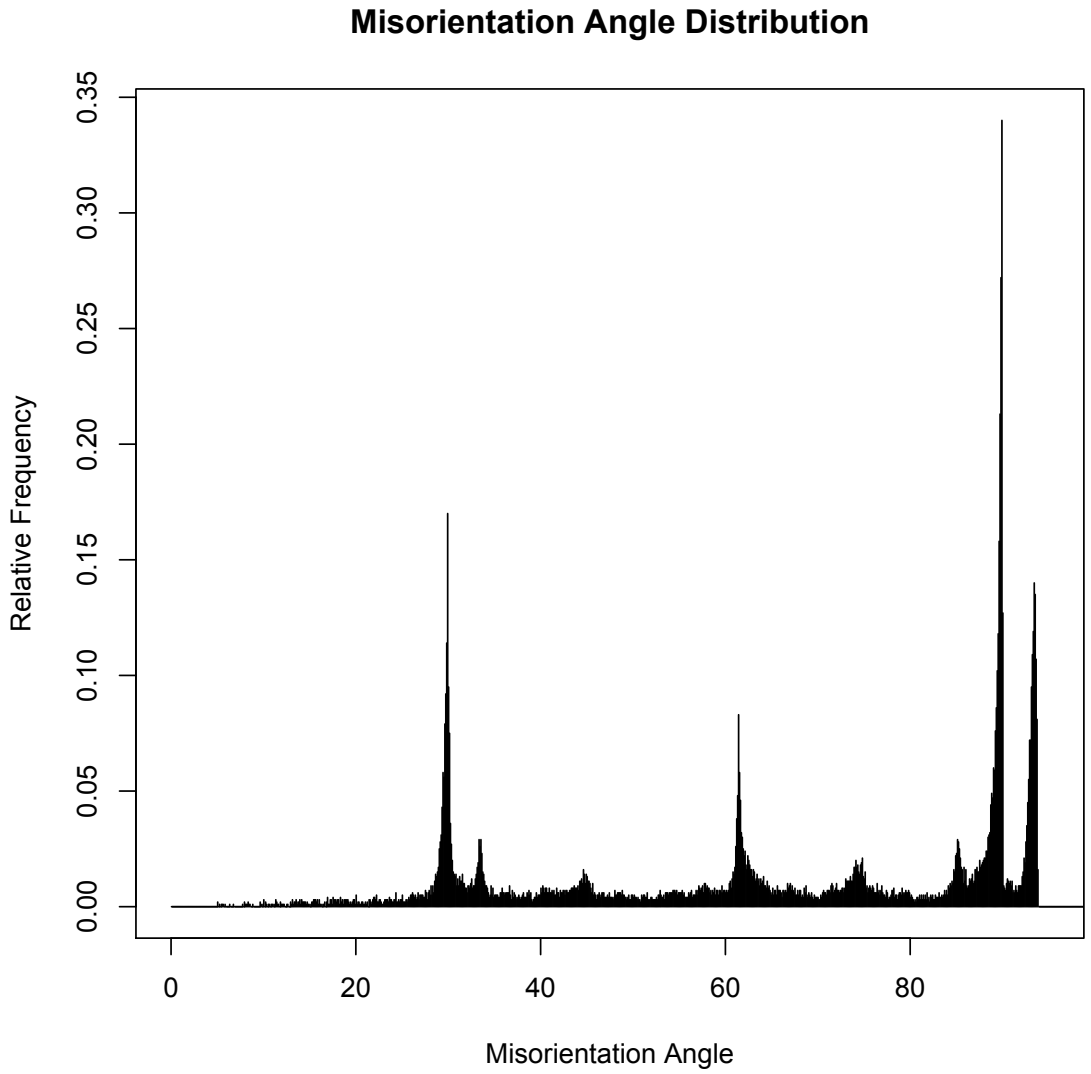

Figure 2: Misorientation angle distribution plot showing large spikes at specific angles. The large spikes in relative frequency correspond to systematic misindexing due to pseudosymmetry. All misorientations 5° or less are considered grain boundaries and are not included in this plot. Data is from JEOL data set, sample 24, scan 1.

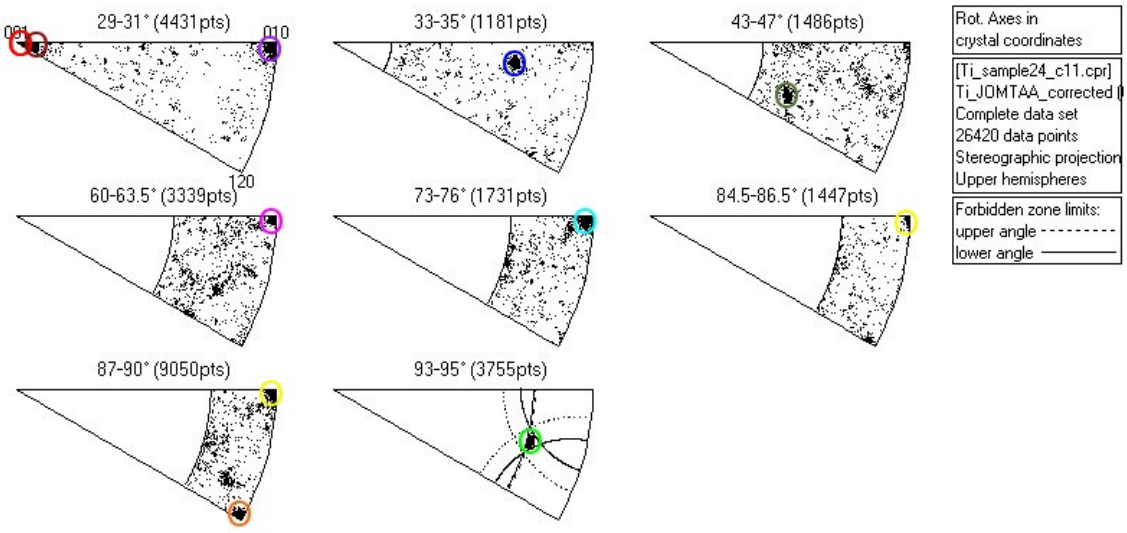

Figure 3 : Misorientation axes plot. The misorientation angle ranges corresponding to the spikes shown in Figure 2 are listed above each of the inverse pole figures. Dark points in the inverse pole figure indicate a large number of misorientations at that location. The location in the inverse pole figures corresponds to misorientation axes. Ten misorientation axes are circled in this figure, with the colors corresponding to the colors described in Table 3. Data is from JEOL data set, sample 24, scan 1.

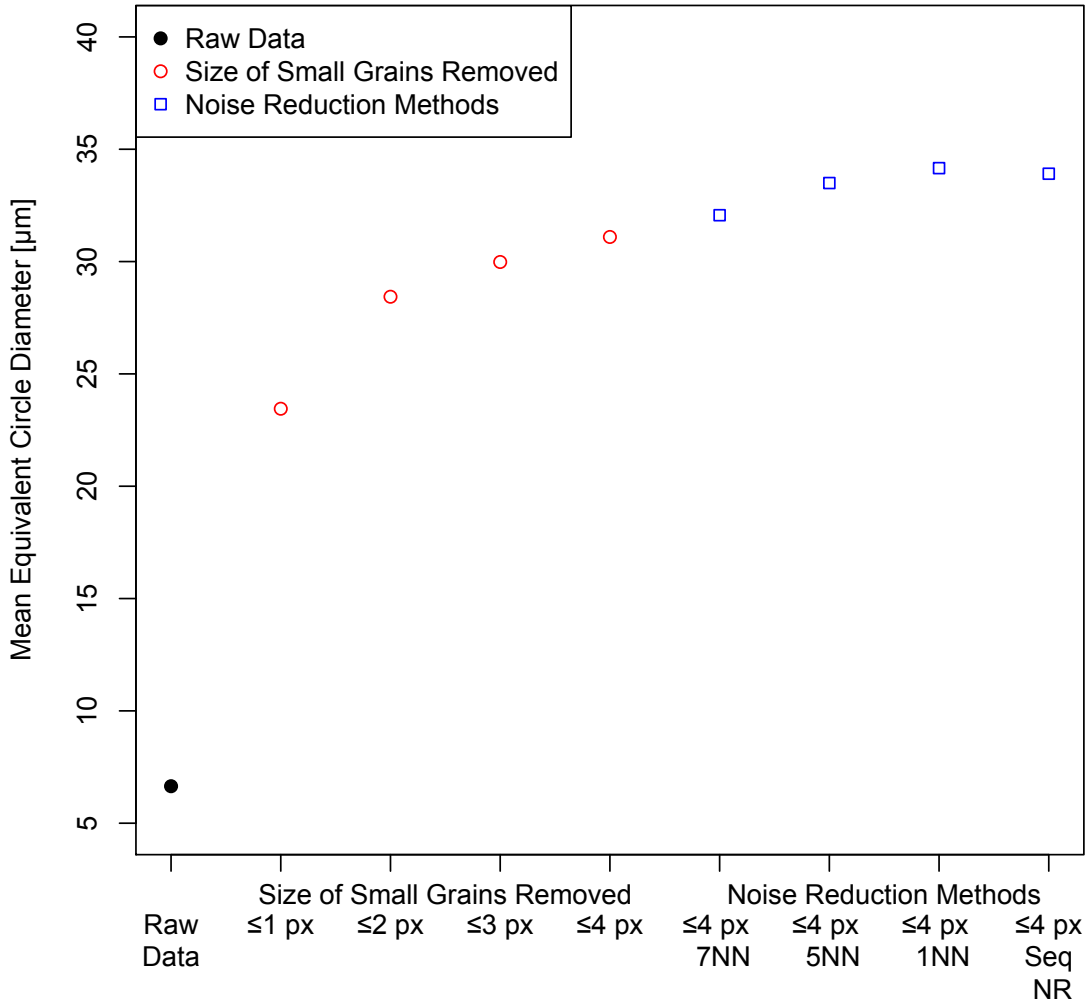

Figure 4: Effect of minimum grain size cutoff (red) and noise reduction methods (blue) on Equivalent Circle Diameter. The grain size from the raw data (black) is also shown. The minimum grain size cutoff values indicate the size grains removed in pixels (px). For the noise reduction methods, all grains four pixels or smaller are removed first. The description 7NN indicates pixels with 7 nearest neighbors (NN) were filled (non iteratively), 5NN indicates pixels with 5 nearest neighbors (NN) were filled (non iteratively), 1NN indicates pixels with 1 nearest neighbor (NN) were filled (non iteratively), Seq NR indicates pixels with 8 NN were filled until no pixels with 8 NN were left, then 7NN iteratively up to 4 NN. Data is from JEOL data set, sample 23, scan 2.

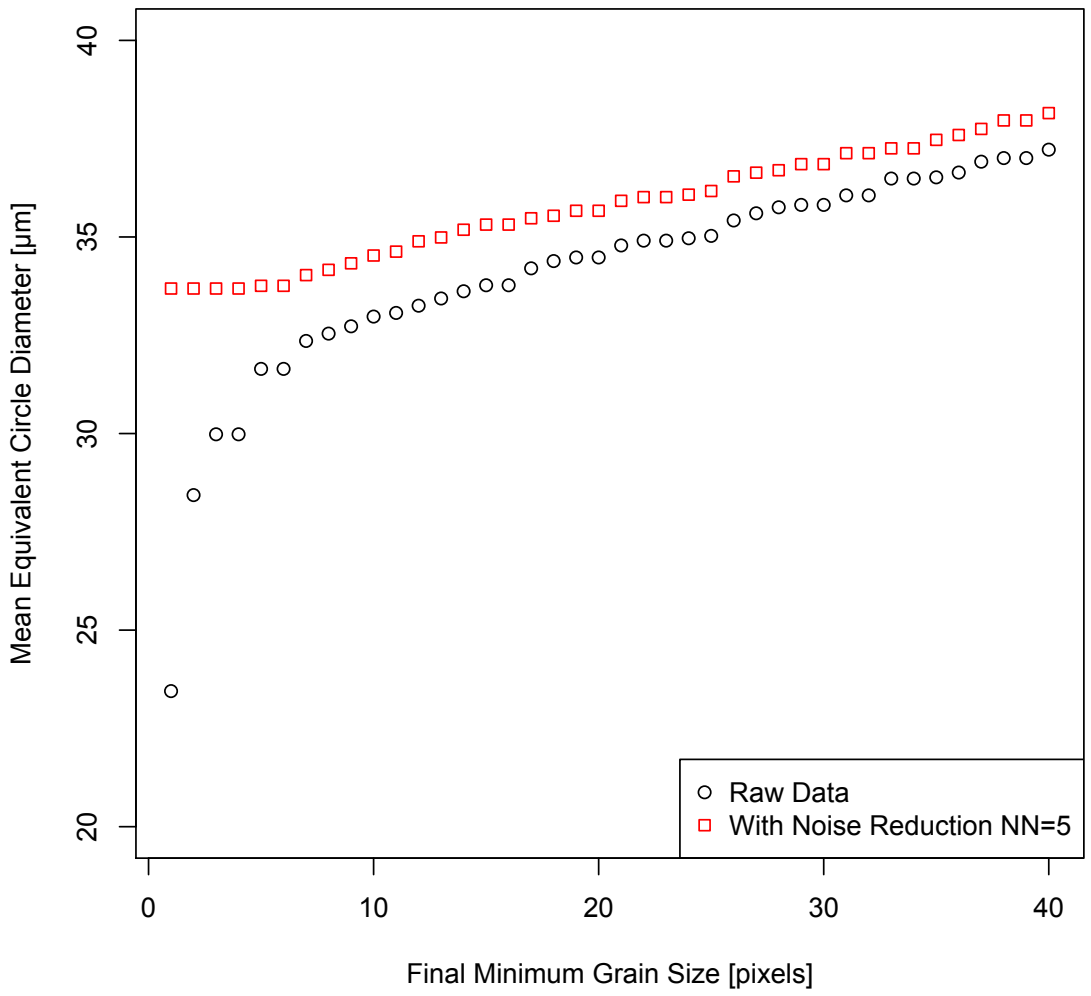

Figure 5: Effect of Final Minimum Grain Size on the Average Grain Size. The average grain size increases nearly linearly depending on final minimum grain size. For the data with noise reduction, the equivalent circle diameter increases at a rate of approximately .13 µm/pixel. Data is from JEOL data set, sample 23, scan 2.

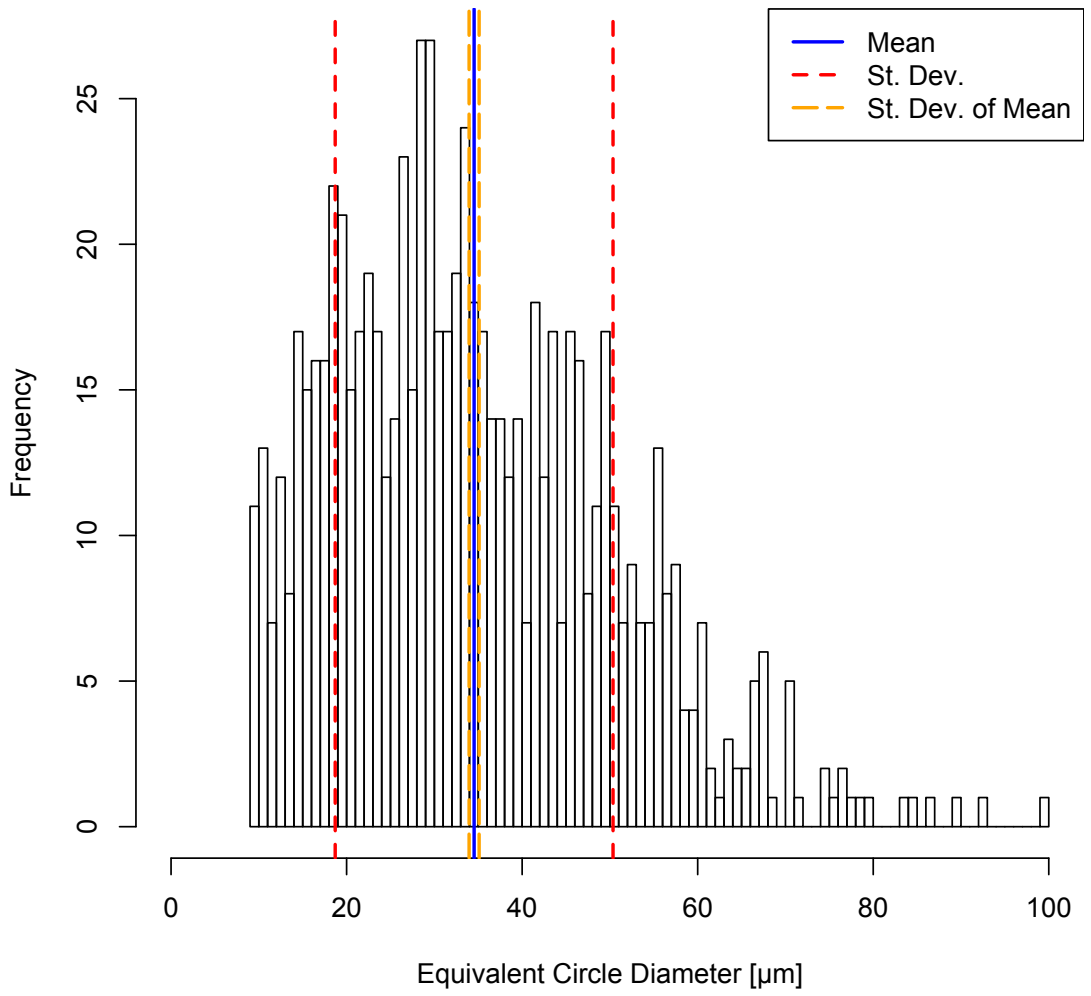

Figure 6: Histogram of the Equivalent Circle Diameter [µm]. The vertical solid blue line is the mean, the vertical dashed red lines are bounds placed one standard deviation on either side, and the vertical dashed orange lines are bounds placed at one standard deviation of the mean. Data are from JEOL data set, sample 23, scan 2.

Tables

Table 1: Calibration measurements for both microscopes used in this study at the working distances and magnifications used for the EBSD grain size analysis. Calibrations were performed in accordance with ISO 16700 using reference material (RM) NIST 8820. Error remains after calibration as a bias error due to a number of factors such as: coupling of x and y calibration values from the requirement of square pixels, truncation of the image from pixelation, drift of the electromagnetic lensing system.

Hitachi 16 May 2011 Working Distance = 18.2mm Magnification=90X		
	Horizontal	Vertical
RM value	1000	750
Mean	1012.6	756.23
Error	1.26%	0.83%
JEOL 6 May 2011 Working Distance = 26mm Magnification = 70X		
	Horizontal	Vertical
RM value	1000	750
Mean	967.6	744.3
Error	3.29%	0.79%

Table 2: Unit cell parameters for hexagonal Ti. b=a, α=β=90°, γ=120°

	a	c	Reference
Ti-Hex	2.95	4.73	HKL Software
Ti-JOMTAA	2.94	4.68	[8]
Ti-PPSOAU	2.951	4.684	[9]

Table 3: Pseudosymmetry operations found in hexagonal Ti samples. Active designates whether the pseudosymmetry operator was used in the grain size analysis. Axis and angle describe the misorientation axis and angle. The tolerance is the angular deviance allowed to axis and angle pairs to still be considered as part of the misorientation axis and angle set. The tolerance applies to both the axis and angle. The colors correspond to the circles in Figure 3.

Active	Axis	Angle	Tolerance	Color
Y	0001	30°	2°	Red
N	-1-120	90°	5°	Yellow
Y	-1010	90°	2°	Orange
Y	16 6 3	92°	2°	Green
N	2 -1 -1 0	72°	5°	Aqua
N	-8 1 2	33°	3°	Blue
N	-1 2 -1 0	30°	3°	Purple
Y	-1 2 -1 0	62°	2°	Pink
N	-1 -1 4	30°	3°	Maroon
N	-1 -3 1	45°	2°	Olive

Table 4: Sample 23 circle equivalent diameter mean grain size (μm)

Area	1	2	3	4	5	Unweighted Average	Standard Deviation	Mean of full dataset
JEOL	34.08	34.53	33.32	33.65	32.93	33.70	0.63	33.69
Number of grains	749	768	787	748	805		Total=	3857
Hitachi	36.64	34.25	36.08	34.94	34.43	35.27	1.05	35.21
Number of grains	614	724	653	686	713		Total=	3390

Table 5: Sample 23 mean linear intercept (μm)

Area	1	2	3	4	5	Unweighted Average	Standard Deviation	Mean of full dataset
JEOL	30.20	30.60	29.23	29.82	29.19	29.81	0.61	29.86
Number of grains	749	768	787	748	805		Total=	3857
Hitachi	32.47	30.36	31.98	30.97	30.51	31.15	0.93	31.15
Number of grains	614	724	653	686	713		Total=	3390

Table 6: Sample 24 circle equivalent diameter mean grain size (μm)

Area	1	2	3	4	5	Unweighted Average	Standard Deviation	Mean of full dataset
JEOL	40.29	34.59	33.59	35.74	35.86	36.01	2.56	35.77
Number of grains	531	711	740	675	672		Total=	3329
Hitachi	34.08	36.51	34.04	33.68	35.39	34.74	1.18	34.56
Number of grains	664	666	735	768	684		Total=	3589

Table 7: Sample 24 mean linear intercept (μm)

Area	1	2	3	4	5	Unweighted Average	Standard Deviation	Mean of full dataset
JEOL	35.70	30.65	29.77	31.68	31.78	31.92	2.27	31.70
Number of grains	531	711	740	675	672		Total=	3329
Hitachi	30.20	35.36	31.36	30.17	29.85	31.39	2.29	30.63
Number of grains	664	666	735	768	684		Total=	3589

Appendices

Appendix A Scan parameters (* indicates these were adjusted before each scan)

[ProjectionParameters]

VHRatio=0.77800
*PCX=0.49800
*PCY=0.86900
*DD=0.43800

[AOI2DHough]
*X0=97
*Y0=62
*R=61

[AOI3DHough]
*Left=36
*Top=1
*Right=158
*Bottom=123

[Band Detection]
Detect=0 (band centers)
Divergence=2 (high)
Min=4
Max=5
HoughRes=80

[Discriminators]
BC=0
BS=0
MAD=5.00000

[Live EBSP]

MinTimePerFrame=9
BackgroundMode=0
AutoBackgroundLevel=10
NoFramesBackGround=50
NoFrames=2
BackgroundCorrOn=True
AutoBackgroundOn=True
AutoStretch=True
Binning=8x8 superfast
Gain=Low
Magnification=70
kV=30.00
TiltAngle=70.00
TiltAxis=90.00
GridDistX=2.5000

xCells=400
yCells=400

Appendix B Data Analysis Methods & Clean up procedure

1) Open data file in Project Manager using Grainsize_ISO profile
   a) Export as .ctf
2) Open data file in Tango
   a) Export Euler Map to results directory
   b) Export Limited Band Contrast Special Boundaries Map to results directory
3) Detect Grains
   a) Sort by area
   b) Select grains 4 pixels or less (0um^2 to 25um^2)
   c) RClick in selected grains -> Into current subset, selected grains
   d) Name '4px or less'
4) Nullify 4px or less subset
   a) Click on '4px or less' subset in project manager (PM)
   b) On subset tab, click nullify - does operation 6.3.1
   c) Click on 'complete' subset in PM
   d) Refresh tango (ctrl-R)
5) Perform Noise Reduction
   a) Extrapolate using 5 nearest neighbors (once) - does operation 6.3.2
   b) Click apply
6) Detect Grains
   a) Sort by area
   b) Select grains 10 pixels or less (0um^2 to 62.5 um^2)
   c) RClick in selected grains -> Into current subset, selected grains
   d) Name '10px or less'
7) Nullify 10px or less subset
   a) Click on '10px or less' subset
   b) On subset tab, click nullify - does operation 6.3.4
   c) Click on 'complete' subset in PM
   d) Refresh tango
8) Export Maps w/ "_cleaned" to filename
   a) Euler Map
   b) Limited Band Contrast Special Boundaries Map
9) Detect Grains
   a) Select grain size statistics
   b) Rclick in window-> "Range to subset"
   c) Name "no border"
   d) Click on "no border subset"
   e) Refresh tango
10) Export Maps w/ "_noborder" to filename
   a) Make sure 'anti-subset' is checked
   b) Euler Map
   c) Limited Band Contrast Special Boundaries Map
11) Detect Grains
   a) RClick - export all cells to file
   b) Comes out as a tab delimited text file
   c) TRUE/FALSE indicates if the grain is a border grain
12) Grain size statistics
   a) Choose size parameter d[um]
   b) Record Ex, N

Appendix C Comments for revising ISO 13067

General comments:

The high hit rate required means ISO 13067 users must know how to optimize their SEM for this measurement. The authors needed to work closely with our application support specialist to get the 90% to 95% hit rate required by ISO 13067, even with optimal sample preparation performed prior to sample arrival.

In our experience both SEMs needed about 1-2 hours of warm up time before it was stable enough to record data. The JEOL would remain stable for long periods (days), while the Hitachi would start to become unstable again after 6-10 hours.

We were not able to set the grain size measurement as an array of measurements (i.e. automatic stage mapping without attempting to overlap the images), we found there were little tweaks necessary in the EBSD geometry, SEM focus or EBSD calibration that if not performed for each area of interest would decrease the hit rate between 5% to 10%.

There is a lot of dispersion in the grain size, so calculation of the uncertainty in the average grain size seems to require repeated measurements, which aren't stated as being required in ISO 13067. Section 5.5.3 alludes to repeated measurements, but does not explicitly require it. Metrics such as standard deviation of the mean may be useful as an alternative to repeated measurements.

When the histograms for frequency vs. grain size are examined, it's pretty obvious that the plot is non-Gaussian. Terms like 'mean' and 'standard deviation' may not have the meaning expected from Gaussian statistics. Better metrics, like those used for log-normal or weibull distributions may be more appropriate.

The EBSD technique allows measurement of the distribution of grain sizes, not just the average value. The distribution data can give much more information than an average, the authors believe ISO 13067 should be revised or a new standard written to measure the distribution of grain sizes.

It may be worth noting in ISO 13067 that the average linear intercept cannot be calculated from the mean average area, the linear intercept needs to be calculated separately for each area and then averaged.

As written, Section 8: Reporting of analysis results, does not explicitly require any mention of the average grain size result, and reporting the data cleaning operations appear to be optional to report.

Specific comments:

3.3.3 – The EBSD patterns are in the SEM reference frame; it's up the user to get them in the sample reference frame.

5.1.1 – This section discusses a threshold of 10% misindexed points, but 6.3.2 states only 5% should be altered. This implies that we will not correct 5% of the misindexed points.

6.1.3 – The authors do not think the qualifier 'easily' should be included with the description of defining twin boundaries, particularly after our difficulties with pseudosymmetry in this sample.

6.3.2 - Is the increase in hit rate stated here relative to the raw data or after step 6.3.1 where small grains are removed? The authors have taken it to be relative to the raw data set, as the small grain removal caused the hit rate to decrease from near 90% to approximately 80%.

6.3.2 - Examples of data with excessive artifacts in the index would be helpful.

6.3.4 - This step seems like a repeat of 6.3.1. After doing the procedure, the authors can see that isn't the case, but seems like a likely place where someone would merge the two steps to save time. A note on why this is a two-step procedure would be good.

6.5 - Should we use geometric mean or arithmetic mean values, since the distribution is non-Gaussian? Arithmetic mean is tacitly implied, but geometric mean might be more applicable.